EUROPEAN ORGANIZATION FOR NUCLEAR RESEARCH

CERN-PPE/96-115
19 August 1996

A measurement of the energy loss spectrum of 150 GeV muons in iron

RD 34 collaboration

E. Berger, R. Blair, J. Dawson, T. Fuess, V. Guarino, N. Hill, S. Magill, E. May, L. Nodulman, L. Price, J. Proudfoot, R. Stanek, D. Underwood, R. Wagner, B. Wicklund
Argonne National Laboratory, USA

G. Blanchot, M. Bosman, P. Casado, M. Cavalli-Sforza, I. Efthymiopoulos, Yu. Ivanyushenkov, A. Juste, Ll. Miralles, S. Orteu, C. Padilla, J.A. Perlas, I. Riu, B. Ronceux, F. Teubert
Institut de Fisica d'Altes Energies, Universitat Autonoma de Barcelona, Spain

K. Anderson, E. Blucher, H. Evans, F. Merritt, J. Pilcher, H. Sanders, M. Shochet, F. Tang, A. Turcot, D. Wagner
University of Chicago, USA

R. Arsenescu, S. Constantinescu, C. Blaj, V. Boldea, S. Dita
Institute of Atomic Physics, Bucharest, Rumania

Z. Ajaltouni, F. Badaud, N. Bouhemaid, P. Brette, M. Brossard, R. Chadelas, J.-C. Chevaleyre, M. Crouau, F. Daudon, J.-J. Dugne, B. Michel, G. Montarou, G.S. Muanza, D. Pallin, H. Plothow-Besch, S. Poirot, G. Reinmuth, L.-P. Says, F. Vazeille
LPC Clermont–Ferrand, Université Blaise Pascal / CNRS–IN2P3, France

M. Cobal, O. Gildemeister, M. Nessi, A. Henriques, L. Poggioli, P. Sonderegger, G. Karapetian
CERN, Geneva, Switzerland

A. Astvatsaturov, O. Borisov, J. Budagov, I. Chirikov-Zorin, G. Chlachidze, V. Glagolev, S. Kakurin, V. Kolomoets, V. Kovtun, V. Kukhtin, A. Lebedev, I. Liba, O. Lomakina, Yu. Lomakin, S. Malyukov, I. Minashvili, D. Pantea, O. Pukhov, V. Romanov, N. Russakovich, V. Senchishin, A. Semenov,

A. Sissakian, A. Shchelchkov, V. Shevtsov, S. Studenov, S. Tokar, N. Topilin,
V. Vinogradov, S. Vorozhtsov, G. Yarygin
JINR Dubna, Russia

F. Cogswell, R. Downing, D. Errede, S. Errede, M. Haney, V. Simaitis, J. Thaler
University of Illinois, USA

P. Amaral[a], A. Amorim[a], J. Carvalho[b], M. David[a], A. Gomes[a], A. Maio[a],
J. P. Martins[a], A. Onofre[b], H. Wolters[c]
*a-LIP and FCUL-Univ. Lisbon, b-LIP and FCTUC-Univ. Coimbra, c-Univ.
Cat. Figueira da Foz, Portugal*

C. Bromberg, J. Huston, R. Miller, R. Richards, C. Yosef
Michigan State University, USA

A. Alifanov, A. Bogush, V. Golubev, V. Rumyantsev, Y. Kulchitsky
Institute of Physics ASB, Minsk, Belarus

C. Angelini, D. Autiero, V. Cavasinni, D. Costanzo, A. De Santo, T. Del Prete,
B. Di Girolamo, V. Flaminio, S. Lami, C. Lazzeroni, E. Mazzoni, G. Renzoni
Pisa University and INFN, Pisa, Italy

T. Davidek, J. Dolejsi, Z. Dolezal, R. Leitner, K. Soustruznik, M. Suk, P. Tas,
Z. Trka, S. Valkar, M. Zdrazil
Charles University, Prague, Czech Republic

M. Lokajicek, S. Nemecek
Academy of Science, Prague, Czech Republic

A. Karyukhin, V. Klyukhin, Yu. Khokhlov, S. Kopikov, M. Kostrikov,
M. Kulagin, V. Lapin, Y. Protopopov, V. Sidorov, A. Solodkov, E. Starchenko,
A. Surkov, A. Zaitsev
Institute for High Energy Physics, Protvino, Russia

L. Caloba, M. Gaspar, F. Marroquin, A. Pereira, J.M. Seixas,
COPPE/EE/UFRJ, Rio de Janeiro, Brazil

S. Berglund, C. Bohm, E. Johansson, S. Hellman, S. Holmgren, K. Jon-And,
B. Sellden, S. Tardell, N. Yamdagni
Stockohlm University, Sweden

A. Ferrer, P.F. Honoré, F. Albiol
IFIC Valencia, Spain

K. De, E. Gallas, J. Li, L. Sawyer, R. Stephens, M. Turcotte, A. White
University of Texas at Arlington, USA

H. Hakopian, V. Grabsky, E. Mnatsakanian, A. Vartapetian
Yerevan Physics Institute, Armenia

Abstract

The energy loss spectrum of 150 GeV muons has been measured with a prototype of the ATLAS hadron calorimeter in the H8 beam of the CERN SPS. The differential probability dP/dv per radiation length of a fractional energy loss $v = \Delta E_\mu / E_\mu$ has been measured in the range $v = 0.01 \div 0.95$; it is then compared with the theoretical predictions for energy losses due to bremsstrahlung and production of electron-positron pairs or of energetic knock-on electrons.
The integrated probability $\int_{0.01}^{0.95} (dP/dv) dv$ is $(1.610 \pm 0.015_{stat.} \pm 0.105_{syst.}) \cdot 10^{-3}$ in agreement with the theoretical predictions of $1.556 \cdot 10^{-3}$ and $1.619 \cdot 10^{-3}$.

Agreement with theory is also found in two intervals of v where production of electron-positron pairs and knock-on electrons dominates.

In the region of bremsstrahlung dominance ($v = 0.12 \div 0.95$) the measured integrated probability $(1.160 \pm 0.040_{stat} \pm 0.075_{syst}) \cdot 10^{-4}$ is in agreement with the theoretical value of $1.185 \cdot 10^{-4}$, obtained using Petrukhin and Shestakov's [11] description of the bremsstrahlung process. The same result is about 3.6 standard deviations (defined as the quadratic sum of statistical and systematic errors) lower than the theoretical prediction of $1.472 \cdot 10^{-4}$, obtained using Tsai's [8] description of bremsstrahlung.

1 Introduction

The search for heavy Higgs bosons via their decay to Z and W pairs at the Large Hadron Collider requires detecting muons with energies in excess of 100 GeV. It is well known that in this regime the energy loss of muons in iron or higher z materials is dominated by radiative effects. In the ATLAS[1] detector muons will be measured by tracking chambers within a toroidal air core magnet after crossing more than 100 radiation lengths of material in the electromagnetic and hadronic calorimeters. It is therefore useful to precisely check the theoretical predictions for muon energy losses in such materials.

Energy losses of muons at very high energies, up to 10 TeV, have been measured in cosmic ray experiments[2, 3, 4]. In these experiments muon energies were measured with a magnetic spectrometer and reasonable agreement between data and calculations was found, except in the region of very small energy losses[4]. Energy losses of muons up to 200 GeV were measured in various accelerator experiments. The measurements of the EMC collaboration [5] are in the region of bremsstrahlung dominance and good agreement was found with Tsai's[8] description of this process. The data of the BCDMS collaboration[6] as well as the results of the Siegen group[7] agree well with the calculations[9] based on the Kokoulin and Petrukhin[10] pair production formula and the Petrukhin and Shestakov[11] expression for bremsstrahlung. It was pointed out by Tannenbaum[12] that Tsai's description of bremsstrahlung differs from Petrukhin's and Shestakov's calculations by approximately 20%. In the same paper the lack of precise measurements in the region of bremsstrahlung dominance (large fractional energy losses) is mentioned.

In this paper, a measurement performed in 1995 with 150 GeV muons incident on a prototype of the ATLAS Tile Calorimeter is described and the results are compared with theoretical predictions. For 150 GeV muons, the dominant energy loss process in the region from 1.5 to 5 GeV is expected to be electron-positron pair production, while energetic knock-on electrons dominate from 5 to 20 GeV and photons from bremsstrahlung dominate the loss spectrum above 20 GeV. Therefore measuring the spectrum between 1.5 and 150 GeV allows to check the contributions from all three processes.

2 Experiment and Data Analysis

The ATLAS Tile Calorimeter is an iron-scintillator sampling calorimeter with wavelength-shifting fiber readout. An important feature of this calorimeter is that the scintillator tiles are placed perpendicular to the colliding beams; a detailed description of the calorimeter concept and of the prototypes is given elsewhere [13]. For the purpose of this measurement, the calorimeter was placed on the H8 beam of the CERN SPS, and oriented so that particles cross the tiles at

perpendicular incidence (along the z-axis on Fig. 0). In this configuration the muon beam traverses alternating layers of iron (14mm) and scintillator (3 mm); this relatively fine granularity gives a resolution of $\sigma/E = 24\%/\sqrt{(E[GeV])}$ for electromagnetic showers. The fibers collecting light from the scintillator are read out by photomultipliers and are grouped to define five layers, each approximately 20 cm thick and containing 8.8 radiation lengths (X_0) of iron. In the experimental setup, five calorimeter modules were stacked on top of each other, and the beam entered in the center of the second, the third (central) or the fourth module. Walls of scintillator detectors [14] was placed on the upstream and downstream sides of the calorimeter.

The momentum-analyzed muon beam, with an energy $E_\mu = 150$ GeV, was defined by three scintillator hodoscopes; the direction of incidence was measured by a pair of two-coordinate wire chambers. Approximately 550,000 muon triggers were used in this analysis.

To suppress triggers with more than one entering particle a minimum-ionizing particle signal was required in scintillator hodoscopes and in the upstream scintillator wall. Hadron contamination was eliminated by cuts on the impact point and on the divergence of the beam together with the requirement that more than 95% of the signal be contained in the central module.

The electron contamination of the beam from muon decay was estimated to be negligible because the mean decay length of 150 GeV muons to electrons is about 10^6 m. The energy spectrum of electron candidates defined as events with zero signals (compatible with pedestals) in the last layer ($35.2 \div 44$ X_0) of the calorimeter and in the downstream scintillator wall is shown on Fig. 1. As expected, the electron contamination is very low and its maximum signal is in the 1^{st} layer of the calorimeter. Few events with energies of about 150 GeV having maximum signal in the 2^{nd} layer was also found in the data. The numbers of events are compatible with the Geant Monte Carlo prediction that about 70% of electron induced showers with the energy of 150 GeV gives maximum signal in the 1^{st} layer of the calorimeter and 30% of showers has its maximum in the 2^{nd} layer. After the contamination cuts, a sample of about 465,000 muon events is left.

In order to ensure full containment of electromagnetic showers produced by muon radiation or knock-on electrons and to suppress the electron background, only events with maximum response in the 2^{nd} or 3^{rd} layer (seen by the beam) of the calorimeter were selected and $v_{max} = 0.95$ (142.5 GeV) was set as the upper limit of studied interval of fractional losses. In order to calculate the effective length L_{eff} over which showers with energy E_{shower} (measured as described below) would be accepted with this selection method, the earliest and latest starting points (x_{min} and x_{max}) of showers with the largest signal in the 2^{nd} or 3^{rd} layer were calculated using a well-known parametrization [15] of the longitudinal profile of the energy deposition of electromagnetic showers

$$dE/dx \propto x^{\alpha(E_{shower})} \cdot e^{-\beta(E_{shower})x}.$$

The difference $L_{eff}(E_{shower}) = (x_{max} - x_{min})/X_0$ is shown in Fig. 2 as function of the fractional energy loss $v = \Delta E_\mu / E_\mu$; it can be seen that L_{eff} is rather precisely given by the thickness of two calorimeter layers (17.6 X_0) up to about 90 GeV ($v = 0.6$), while for higher energy losses the effective length decreases (due to the logarithmic longitudinal growth of showers) by at most 3%. L_{eff} above 90 GeV is well described by

$$L_{eff}(E_{shower}) = 17.6 - \ln(E_{shower}[GeV]/90)$$

Acceptance calculations were crosschecked by GEANT 3.21 Monte Carlo simulations (which include muon radiative losses and knock-on electron production); the simulations confirm the analytical result, with larger errors for large muon energy losses.

The energy E_{shower} lost by muons in the calorimeter is defined in this analysis excluding the low-energy-ionization signal. It was calculated by summing the signals in two to four consecutive layers and subtracting the most probable muon signal E_{mp} in those layers. All consecutive layer signals in excess of $E_{mp} + 3\sigma_{mp}$ were summed to obtain E_{shower} (see Fig. 3). This method minimizes the correction from the low energy ionization produced by muons and the error from its fluctuation. These corrections are important for the lowest energy losses: for instance, for $E_{shower} = 1.5$ GeV the muon ionization signal is almost $0.3E_{shower}$ therefore it is imperative to subtract it from the total signal.

The subtraction procedure was also simulated using GEANT 3.21, in order to estimate the contribution of events with more than one shower to the differential probability distribution. 100,000 muons traversing the calorimeter structure were simulated; for each event the energy lost by muons in each of 55 iron and scintillator slabs together with the energy losses of electrons and positrons in the scintillators were recorded. Differential probability distributions obtained by forming the E_{shower} sum with different subtraction procedures were compared with the distribution of the largest single energy loss in one iron slab (0.8 X_0), because the latter distribution can be directly compared to the theoretical results. Subtracting E_{mp} the expected contribution of multiple shower events to dP/dv is 25%, 6% and 0% for $v = 0.01, 0.1$ and 1. respectively, as shown in Fig. 4. In the Figure one may also see that subtraction of a truncated mean of the muon signal (1.6 times the most probable signal) fully eliminates multiple shower contributions. The two methods – subtraction of the most probable signal followed by correction of dP/dv and subtraction of the truncated mean signal - give a difference in the total integrated energy loss probability of $\pm 0.3\%$ which was included in the estimate of the systematic error.

The signal energy scale, *i.e.* the conversion factor to obtain the energy of the signals from the digitized photomultiplier signals, was not independently known to sufficient accuracy and was therefore obtained from the data by several methods.

- The signal/energy conversion factor was varied to obtain the best fit to the theoretical distribution of muon energy losses (see Sect. 3). The main effect of this procedure essentially is to set the energy of the endpoint of the experimental distribution to the muon beam energy; the conversion factor thus obtained is quite insensitive to the integral of the energy loss spectrum and its detailed shape.

- The conversion factor was calculated by requiring that the integral of the spectrum agree with theory.

- In the central region between 7.5 and 30. GeV (v=0.05 to 0.2) where the data corrections are low and the difference of theoretical descriptions is still below $\pm 3\%$ the integrated probability was adjusted to its theoretical value.

- The mean energy loss in the central region of v was fitted to the theoretical prediction. This method is insensitive to the common normalization factor.

To minimize the dependance of results on theory the mean value of the conversion factor obtained by the first and the last methods was used in the analysis. The other methods gave conversion factors differing by $\pm 3\%$. This value was used for the estimate of systematic errors.

The lower limit of the analyzed energy loss spectrum was set to 1.5 GeV because for this value the signal from the processes studied in this paper is sufficiently well separated from the most probable muon signal:

$$E_{mp} + 3\sigma_{mp} \leq E_{shower} - 3\sigma_{shower}\,,$$

(where $\sigma_{shower}[GeV] = 0.24 \cdot \sqrt{E_{shower}[GeV]}$) for $E_{shower} \geq 1.5$ GeV.

Finally the differential probability per radiation length of a fractional energy loss in the i-th interval was calculated as

$$\frac{\Delta P}{\Delta v} = \frac{(N_i/N_{tot})}{\Delta v_i} \cdot \frac{1}{L_{eff}(\langle v \rangle_i)}$$

where N_i is the number of events in the $i-$th interval, N_{tot} is the total number of events passing the cuts, Δv_i is the width of the $i-$th interval, $L_{eff}(\langle v \rangle_i)$ is the effective length for the mean $\langle v \rangle_i$ of that interval.

The measured differential probabilities per radiation length of iron are given in Table 1 and are plotted in Fig. 7. The errors quoted are statistical only. The systematic errors of the energy loss spectrum are dominated by the uncertainty on the signal energy scale, which we take to be $\pm 3\%$, by the uncertainty on the muon energy ($\pm 1.5\%$) and by the uncertainty on the iron sbsorber thickness ($\pm 1.0\%$). Because the systematic errors are correlated, the data have been processed with different values of the signal energy scale, of the muon energies and of absorber thickness and the maximal positive and negative deviations of mean values were

taken as systematic errors. The result is an overall systematic error on the differential probability of fractional energy loss dP/dv of $\pm$ 7%, which dominates the results in the low energy region, but is comparable to the statistical errors in the high energy region (see Fig. 7).

3 Theoretical Predictions

The theoretical predictions to be compared to these results are discussed next. The analytical expressions are given in full in order to facilitate comparisons.

Pair production: Kel'ner's and Kotov's[16] expression for the differential probability per radiation length of muon energy loss by pair production is

$$\left(\frac{dP}{dv}\right)_{pair} = C\frac{16}{\pi}Z^2\alpha^2\frac{1}{v}F(E_\mu, v). \qquad (1)$$

The constant C is given by $C = X_0\rho\frac{N_A}{A}r_e^2 = 1.185 \cdot 10^{-2}$.
Here N_A is the Avogadro number, r_e is the classical electron radius and α is the fine structure constant; X_0, ρ, A and Z are the radiation length, the density, the atomic weight and the atomic number of iron.
The function $F(E_\mu, v)$ is tabulated in [16] for lead and sodium at different muon energies. The interpolation of Kel'ner's and Kotov's function $F(E_\mu, v)$ for the energy loss of 150 GeV muons in iron is shown on Fig. 5 together with the parametrization used in this paper:

$$\ln F_{Fe}(E_\mu = 150\ GeV, v) = -0.175\ln^2(v) - 2.748\ln(v) - 9.736.$$

Knock-on electrons: To describe the production of energetic knock-on electrons, the Bhabha formula [17] given by Rossi[18] is used (m_e is the electron mass and C as defined as above):

$$\left(\frac{dP}{dv}\right)_{knock-on} = C2\pi Z\left(\frac{m_e}{E_\mu}\right)\frac{1 - v + \frac{v^2}{2}}{v^2} \qquad (2)$$

Bremsstrahlung: To compare these results with predictions of muon bremsstrahlung the expression given by Petrukhin and Shestakov[11], and another calculation by Tsai[8] are used.
The expression of Petrukhin and Shestakov

$$\left(\frac{dP}{dv}\right)^{PS}_{bremsstrahlung} = C4Z^2\alpha\left(\frac{m_e}{m_\mu}\right)^2\frac{1}{v}\left(\frac{4}{3} - \frac{4}{3}v + v^2\right)\Phi^{PS}(\delta) \qquad (3)$$

contains the screening function:

$$\Phi^{PS}(\delta) = \ln \frac{\frac{2}{3}\frac{189 m_\mu}{m_e} Z^{-2/3}}{1 + \frac{189\sqrt{e}}{m_e}\delta Z^{-1/3}} \tag{4}$$

where m_μ is the muon mass, $\delta = m_\mu^2 v/2E_\mu(1-v)$ is the minimum momentum transfer to the nucleus and $e = 2.718$. The function $\Phi^{PS}(\delta)$ is an approximation of the exact screening function and is valid within 1% up to δ=0.1m_μ (v=0.9 for $E_\mu = 150\ GeV$)[11].
To compare the previous formula with the differential probability distribution given by Tsai[8, 12], his formula has been written as:

$$\left(\frac{dP}{dv}\right)^{TS}_{bremsstrahlung} = C4Z^2\alpha\left(\frac{m_e}{m_\mu}\right)^2 \frac{1}{v}\left(\frac{4}{3} - \frac{4}{3}v + v^2\right)\Phi^{TS}(\delta) \tag{5}$$

where the screening function $\Phi^{TS}(\delta)$ is :

$$\begin{aligned}\Phi^{TS}(\delta) = \frac{\phi_1(a\delta)}{4} - \frac{1}{3}\ln Z - f_{coul} + \frac{1}{Z}\left(\frac{\psi_1(a'\delta)}{4} - \frac{2}{3}\ln Z\right) \\ + \frac{\frac{2}{3}(1-v)}{\frac{4}{3} - \frac{4}{3}v + v^2}\left(\frac{\phi_1 - \phi_2}{4} + \frac{1}{Z}\frac{\psi_1 - \psi_2}{4}\right)\end{aligned} \tag{6}$$

The functions ϕ_1 and ψ_1 have arguments $a\delta$ and $a'\delta$; $a = 184.15/(\sqrt{e}\ m_e Z^{1/3})$ and $a' = 1194/(\sqrt{e}\ m_e Z^{2/3})$. The two functions are defined for zero momentum transfer:
$\phi_1(0) = 4\ln(\sqrt{e}aZ^{1/3}m_\mu)$, $\psi_1(0) = 4\ln(\sqrt{e}a'Z^{2/3}m_\mu)$
and for an arbitrary δ:
$\phi_1(a\delta) = \phi_1(0) - 2\ln(1 + (a\delta)^2) - 4(a\delta)arctg(1/a\delta)$,
$\psi_1(a'\delta) = \psi_1(0) - 2\ln(1 + (a'\delta)^2) - 4(a'\delta)arctg(1/a'\delta)$.
The asymptotic behavior of ϕ_2 and ψ_2:
$\phi_1(0) - \phi_2(0) = \psi_1(0) - \psi_2(0) = 2/3$
at zero momentum transfer and
$\phi_1 - \phi_2 = \psi_1 - \psi_2 = 0$
for large arguments is fixed by the equations[8]:
$\phi_2(a\delta) = \phi_1(a\delta) - (2/3)/(1 + 6.5a\delta + 6(a\delta)^2)$,
$\psi_2(a'\delta) = \psi_1(a'\delta) - (2/3)/(1 + 40a'\delta + 400(a'\delta)^2)$.
Finally $f_{coul} = 4.197 \cdot 10^{-2}$ is the correction for the Coulomb interaction.

Screening functions for both Petrukhin and Shestakov (Φ^{PS}) and Tsai's (Φ^{TS}) description of bremsstrahlung are plotted on Fig. 6.

Photonuclear interactions: Photonuclear interactions contribute also to the muon energy loss. The probability is given by the following formula[19]:

$$\left(\frac{dP}{dv}\right)_{photonuclear} = C\left(\frac{A\sigma_{\gamma N}(\epsilon)}{\pi r_e^2}\right)\frac{\alpha}{2}v\Gamma(E_\mu, v) \quad (7)$$

where the function $\Gamma(E_\mu, v)$ is given by

$$\begin{aligned}\Gamma(E_\mu, v) &= \frac{3}{4}G(x)\left(\kappa\ln(1+\frac{m_1^2}{t}) - \frac{\kappa m_1^2}{m_1^2+t} - \frac{2m_\mu^2}{t}\right)\\ &+ \frac{1}{4}\left(\kappa\ln(1+\frac{m_2^2}{t}) - \frac{2m_\mu^2}{t}\right)\\ &+ \frac{m_\mu^2}{2t}\left(\frac{3}{4}G(x)\frac{m_1^2}{m_1^2+t} + \frac{1}{4}\frac{m_2^2}{t}\ln(1+\frac{t}{m_2^2}\right) \quad (8)\end{aligned}$$

with

$$\begin{aligned}G(x) &= \frac{3}{x^2}\left(\frac{x^2}{2} - 1 + e^{-x}(1+x)\right)\\ x &= 0.00282A^{1/3}\sigma_{\gamma N}(\Delta E_\mu)\\ \sigma_{\gamma N}(\Delta E_\mu) &= 114.3 + 1.647\ln^2(0.0213\Delta E_\mu[GeV])\ \mu b\\ t &= \frac{m_\mu^2 v^2}{1-v}\\ \kappa &= 1 - \frac{2}{v} - \frac{2}{v^2}\\ m_1^2 &= 0.54GeV^2\\ m_2^2 &= 1.80GeV^2\end{aligned}$$

The contribution of photonuclear interactions is about 1% for the lowest values of the fractional loss v and about 5% for the highest v value (see Fig. 7), but it is suppressed by the selection criteria applied to the data which have been optimized for electromagnetic secondary products. The maximum contributions of photonuclear processes are estimated to be about 0.5% and 2% for the lowest and the highest values of v respectively and have been subtracted from the measured values of dP/dv.

The values of these theoretical expressions over the observed energy loss range are given in Fig. 7; the sum of the differential probabilities from the first three processes are given in the figure and in Table 1. The data can be compared with the calculations of Kel'ner and Kotov for pair production (curve P in Fig. 7), the Bhabha formula for knock-on electrons (K) and with Petrukhin's and Shestakov's (B^{PS}) and Tsai's (B^{TS}) calculations for bremsstrahlung processes.

4 Comparison of Experiment and Theory

The theoretical predictions are in very good agreement with the experimental results over the whole analyzed range of fractional energy loss v from 0.01 to 0.95. It is worth noting that there are no free parameters in the comparison of theory and experiment, except for the very weak coupling introduced by the requirement that the endpoint of the experimental energy loss distribution match the muon energy.

Since different processes dominate in different regions of v, theory and experiment can also be usefully compared in suitably chosen regions of the spectrum. The analyzed range of v can be divided into the three intervals given in Table 2. About 55% of the integrated probability $\Delta P = \int_{v_{min}}^{v_{max}} \frac{dP}{dv} dv$ in the first interval is due to the production of e^+e^- pairs, in the second interval 45% of the integral is due to knock-on electrons and in the third the dominant contribution (60%) comes from bremsstrahlung. The results obtained in all three intervals agree within one standard deviation (defined as the quadratic sum of statistical and systematic errors) with the theoretical predictions of Petrukhin and Shestakov for bremsstrahlung. The integrated probability value $\Delta P_{P+K+B^{Ts}} = 1.472 \cdot 10^{-4}$ in the region $v = 0.12 \div 0.95$ calculated with Tsai's description of bremsstrahlung is about 3.6σ higher than the measured value $\Delta P = (1.160 \pm 0.040_{stat} \pm 0.075_{syst}) \cdot 10^{-4}$. This statement is illustrated further in Fig. 8, in which detailed comparison of the data and theory is shown. It can be seen that the results favor the description of bremsstrahlung by Petrukhin and Shestakov which predicts a lower probability for catastrophic muon losses.

References

[1] ATLAS Collaboration: ATLAS Technical Proposal CERN/LHCC/94-43

[2] W. Stamm et al.: Nuovo Cim. 51A (1979) 242

[3] K. Mitsui et al.: Nuovo Cim. 73A (1983) 235

[4] W.K. Sakumoto et al.: UR-1209 (1991)

[5] J.J. Aubert et al.: Z.Phys. C10 (1981) 101

[6] R. Kopp et al.: Z.Phys. C28 (1985) 171

[7] R. Baumgart et al.: Nucl. Instrum. Methods A258 (1987) 51

[8] Y. Tsai: Rev. Mod. Phys. 46 (1974) 815

[9] W. Lohmann et al. CERN Report 85-03 (1985)

[10] R.P. Kokoulin, A.A. Petrukhin: Acta Phys. Acad. Sci. Hung. 29 Suppl. 4 (1970) 277

[11] A.A. Petrukhin, V.V. Shestakov: Can. J. Phys. 46 (1968) S377

[12] M.J. Tannenbaum: CERN-PPE/91-134 (1991)

[13] F. Ariztizabal et al.: Nucl. Instrum. Methods A349 (1994) 384, E. Berger et al.: CERN/LHCC 95-44

[14] M. Lokajicek et al.: ATLAS Internal Note TILECAL-NO-063 (1995)

[15] Particle Data Group, Phys. Rev. D50 (1994) 1173

[16] S.R. Kel'ner, Yu.D. Kotov: Sov. J. Nucl. Phys. 7 (1968) 360

[17] H.J. Bhabha: Proc. Roy. Soc. A164 (1938) 257

[18] B. Rossi: High Enery Particles, New York: Prentice-Hall 1952

[19] L.B. Bezrukov, E.V. Bugaev: Sov. J. Nucl. Phys. 33 (1981) 635

Figure and Table Captions

Fig 0. The principle of the ATLAS Tile Calorimeter module. The direction of secondary particles produced in future LHC pp collision is shown by arrow "Hadrons". In described experiment, muons cross the tiles at perpendicular incidence along z direction.

Fig 1. The spectrum of the electron contamination of the muon beam.

Fig 2. The length L_{eff} (in radiation lengths of iron) of the muon path in the calorimeter over which showers are accepted by the selection algoritm, as a function of the relative muon energy losses. Full and empty circles are results of simplified and GEANT Monte Carlo calculations respectively.

Fig 3. Example of a 36 GeV electromagnetic shower as seen in the data. The energy E_{shower} is the sum of energies in three consecutive layers (2nd to 4th) with the signal above $E_{mp} + 3\sigma_{mp}$ and with the most probable muon signal E_{mp} subtracted. The arrow corresponds to the direction of the incident muon.

Fig 4. Monte Carlo study of the multiple shower contribution to the differential probability distribution dP/dv. The full circles correspond to fractional losses defined as $v_m = (\Delta E_\mu - E_{m.p.})/E_\mu$, empty circles are for $v_m = (\Delta E_\mu - 1.6 \cdot E_{m.p.})/E_\mu$. The energy loss in one radiative or knock-on process is defined as $v_1 = \Delta E_{max}/E_\mu$ with ΔE_{max} being the largest energy loss in one iron slab ($0.8\ X_0$) in each muon traversal of the calorimeter.

Fig 5. The function $F(E_\mu, v)$ (see formula (1) in the text) for e^+e^- pair production by 150 GeV muons in iron. The points has been obtained by interpolation of values tabulated in Ref. [16].

Fig 6. Comparison of the screening functions by Petrukhin and Shestakov (Φ^{PS}) and Tsai's (Φ^{TS}) description of bremsstrahlung for 150 GeV muons in iron.

Fig 7. The distribution of differential probabilities dP/dv for the energy loss of 150 GeV muons in iron. The curves P, K and B^{PS}, B^{TS} for pair production, knock-on electrons production and bremsstrahlung correspond to eq. (1), (2), (3) and (5) in the text. The full curves are the sum of P, K and B^{PS} (lower one) and P, K and B^{TS} (upper one). The contribution of the energy loss due to photonuclear reactions (PH) is also shown.

Fig 8. Detailed comparison of the data and theory with the Petrukhin and Shestakov description of bremsstrahlung. Hatched and empty rectangles correspond to statistical and systematic errors respectively. The upper curve is the theoretical prediction with Tsai's formula for bremsstrahlung.

Table 1. Comparison of the measured differential probability values $\Delta P/\Delta v$ for fractional muon energy losses with theoretical calculations $(dP/dv)_{P+K+B^{PS}}$ according to the addition of formulae (1), (2) and (3) and $(dP/dv)_{P+K+B^{TS}}$ according to the addition of formulae (1), (2) and (5) in the text. Only statistical errors are quoted. The error of $\langle v \rangle$ is estimated as the r.m.s. value divided by square root of the number of events in a given interval.

Table 2. Integrated probabilities $\Delta P = \int_{v_{min}}^{v_{max}} \frac{dP}{dv} dv$ per radiation length measured in three different intervals (v_{min}, v_{max}) compared with theoretical cal-

culations for the sum of pair production (P), knock-on electron production (K) and two different formulae for bremsstrahlung, (B^{PS}) and (B^{TS}) (see formulae (1),(2),(3) and (5) respectively).

$\langle v \rangle$	$\frac{\Delta P}{\Delta v}$	$(\frac{dP}{dv})_{P+K+B^{PS}}$	$(\frac{dP}{dv})_{P+K+B^{TS}}$
$(1.054 \pm 0.001) \cdot 10^{-2}$	$(1.50 \pm 0.04) \cdot 10^{-1}$	$1.52 \cdot 10^{-1}$	$1.54 \cdot 10^{-1}$
$(1.170 \pm 0.001) \cdot 10^{-2}$	$(1.22 \pm 0.03) \cdot 10^{-1}$	$1.23 \cdot 10^{-1}$	$1.24 \cdot 10^{-1}$
$(1.298 \pm 0.001) \cdot 10^{-2}$	$(1.02 \pm 0.03) \cdot 10^{-1}$	$0.99 \cdot 10^{-1}$	$1.00 \cdot 10^{-1}$
$(1.441 \pm 0.001) \cdot 10^{-2}$	$(9.0 \pm 0.3) \cdot 10^{-2}$	$7.93 \cdot 10^{-2}$	$8.03 \cdot 10^{-2}$
$(1.600 \pm 0.002) \cdot 10^{-2}$	$(6.9 \pm 0.2) \cdot 10^{-2}$	$6.37 \cdot 10^{-2}$	$6.45 \cdot 10^{-2}$
$(1.781 \pm 0.002) \cdot 10^{-2}$	$(5.1 \pm 0.2) \cdot 10^{-2}$	$5.07 \cdot 10^{-2}$	$5.15 \cdot 10^{-2}$
$(1.975 \pm 0.002) \cdot 10^{-2}$	$(4.4 \pm 0.2) \cdot 10^{-2}$	$4.07 \cdot 10^{-2}$	$4.14 \cdot 10^{-2}$
$(2.192 \pm 0.003) \cdot 10^{-2}$	$(3.6 \pm 0.1) \cdot 10^{-2}$	$3.26 \cdot 10^{-2}$	$3.32 \cdot 10^{-2}$
$(2.438 \pm 0.003) \cdot 10^{-2}$	$(2.7 \pm 0.1) \cdot 10^{-2}$	$2.59 \cdot 10^{-3}$	$2.65 \cdot 10^{-3}$
$(2.702 \pm 0.004) \cdot 10^{-2}$	$(2.11 \pm 0.09) \cdot 10^{-2}$	$2.08 \cdot 10^{-2}$	$2.13 \cdot 10^{-2}$
$(2.996 \pm 0.004) \cdot 10^{-2}$	$(1.71 \pm 0.08) \cdot 10^{-2}$	$1.67 \cdot 10^{-2}$	$1.71 \cdot 10^{-2}$
$(3.333 \pm 0.005) \cdot 10^{-2}$	$(1.41 \pm 0.07) \cdot 10^{-2}$	$1.32 \cdot 10^{-2}$	$1.37 \cdot 10^{-2}$
$(3.886 \pm 0.009) \cdot 10^{-2}$	$(9.6 \pm 0.4) \cdot 10^{-3}$	$9.54 \cdot 10^{-3}$	$9.90 \cdot 10^{-3}$
$(4.81 \pm 0.01) \cdot 10^{-2}$	$(5.9 \pm 0.3) \cdot 10^{-3}$	$6.08 \cdot 10^{-3}$	$6.37 \cdot 10^{-3}$
$(5.89 \pm 0.02) \cdot 10^{-2}$	$(4.1 \pm 0.2) \cdot 10^{-3}$	$3.98 \cdot 10^{-3}$	$4.22 \cdot 10^{-3}$
$(7.28 \pm 0.02) \cdot 10^{-2}$	$(2.6 \pm 0.1) \cdot 10^{-3}$	$2.57 \cdot 10^{-3}$	$2.77 \cdot 10^{-3}$
$(9.02 \pm 0.03) \cdot 10^{-2}$	$(1.7 \pm 0.1) \cdot 10^{-3}$	$1.68 \cdot 10^{-3}$	$1.84 \cdot 10^{-3}$
$(1.105 \pm 0.004) \cdot 10^{-1}$	$(1.22 \pm 0.08) \cdot 10^{-3}$	$1.13 \cdot 10^{-3}$	$1.27 \cdot 10^{-3}$
$(1.440 \pm 0.008) \cdot 10^{-1}$	$(7.1 \pm 0.4) \cdot 10^{-4}$	$6.89 \cdot 10^{-4}$	$7.92 \cdot 10^{-4}$
$(1.96 \pm 0.01) \cdot 10^{-1}$	$(3.8 \pm 0.3) \cdot 10^{-4}$	$3.94 \cdot 10^{-4}$	$4.69 \cdot 10^{-4}$
$(2.68 \pm 0.02) \cdot 10^{-1}$	$(2.2 \pm 0.2) \cdot 10^{-4}$	$2.27 \cdot 10^{-4}$	$2.80 \cdot 10^{-4}$
$(3.71 \pm 0.03) \cdot 10^{-1}$	$(1.2 \pm 0.1) \cdot 10^{-4}$	$1.29 \cdot 10^{-4}$	$1.65 \cdot 10^{-4}$
$(5.38 \pm 0.06) \cdot 10^{-1}$	$(6.4 \pm 0.6) \cdot 10^{-5}$	$6.75 \cdot 10^{-5}$	$9.06 \cdot 10^{-5}$
$(7.87 \pm 0.09) \cdot 10^{-1}$	$(3.1 \pm 0.3) \cdot 10^{-5}$	$3.49 \cdot 10^{-5}$	$5.02 \cdot 10^{-5}$

Table 1

Comparison of the measured differential probability values $\Delta P/\Delta v$ for fractional muon energy losses with theoretical calculations $(dP/dv)_{P+K+B^{PS}}$ according to the addition of formulae (1), (2) and (3) and $(dP/dv)_{P+K+B^{TS}}$ according to the addition of formulae (1), (2) and (5) in the text. Only statistical errors are quoted. The error of $\langle v \rangle$ is estimated as the r.m.s. value divided by square root of the number of events in a given interval.

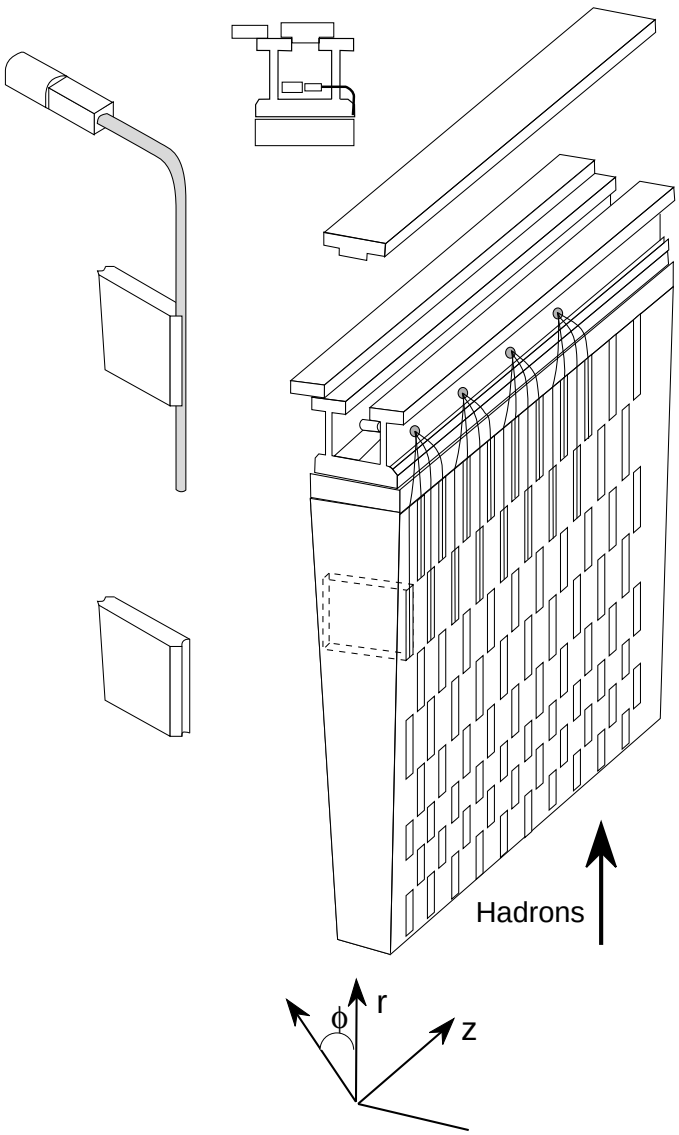

Fig. 0

The principle of the ATLAS Tile Calorimeter module. The direction of secondary particles produced in future LHC pp collision is shown by arrow "Hadrons". In described experiment, muons cross the tiles at perpendicular incidence along z direction.

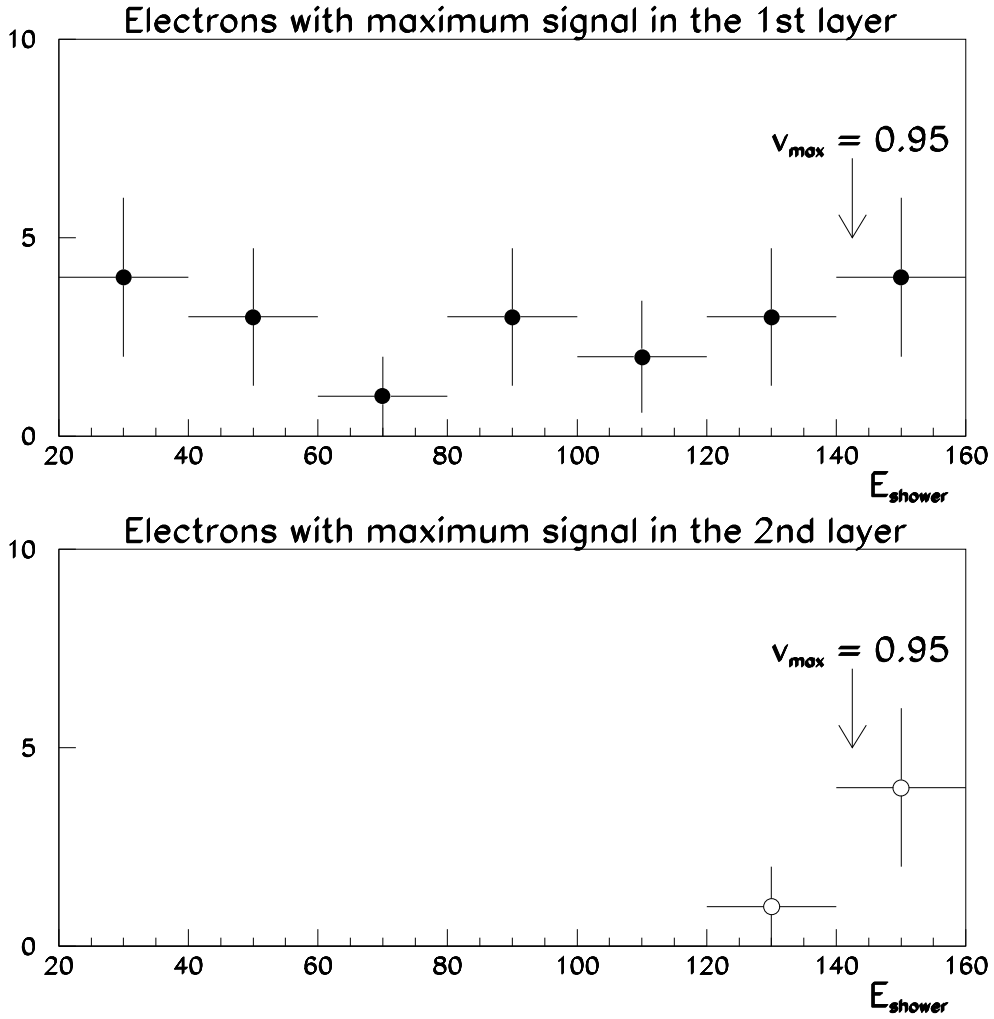

Fig. 1

The spectrum of the electron contamination of the muon beam.

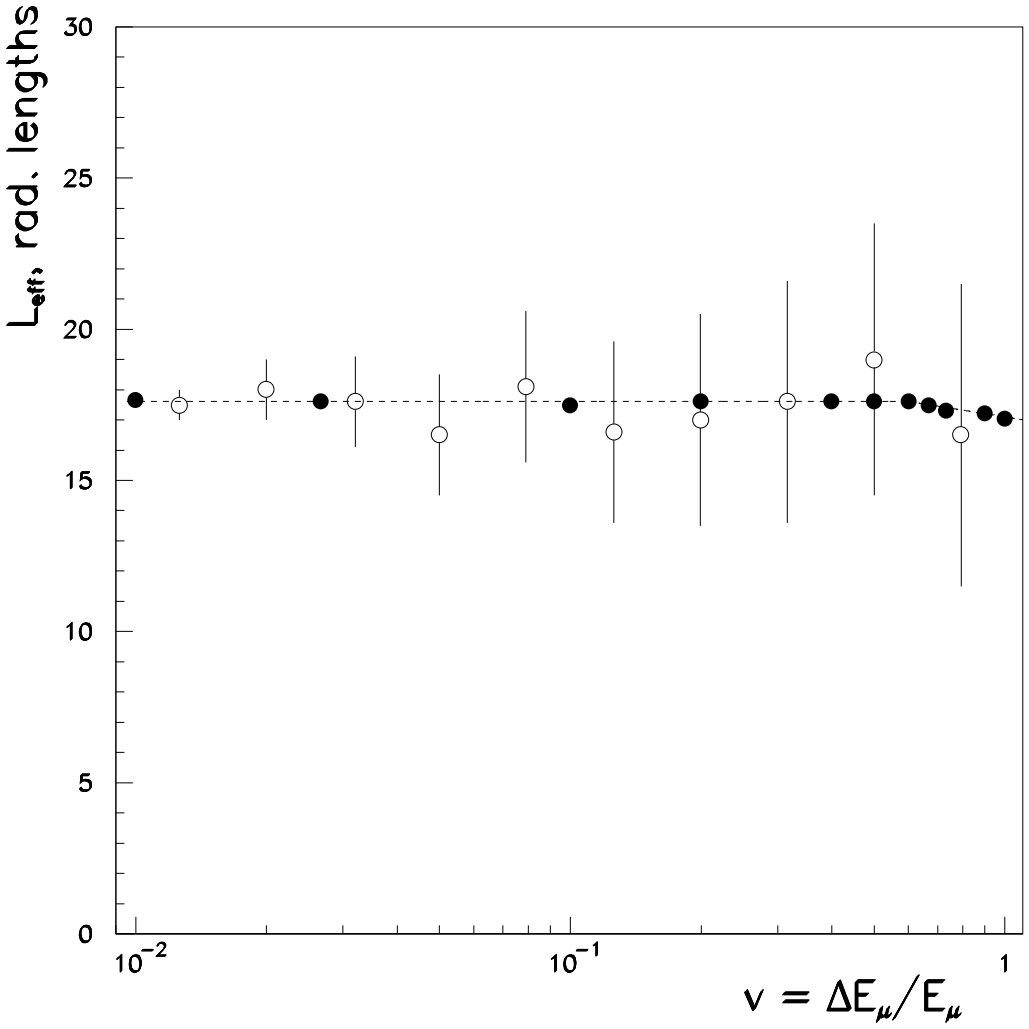

Fig. 2

The length L_{eff} (in radiation lengths of iron) of the muon path in the calorimeter over which showers are accepted by the selection algoritm, as a function of the relative muon energy losses. Full and empty circles are results of simplified and GEANT Monte Carlo calculations respectively.

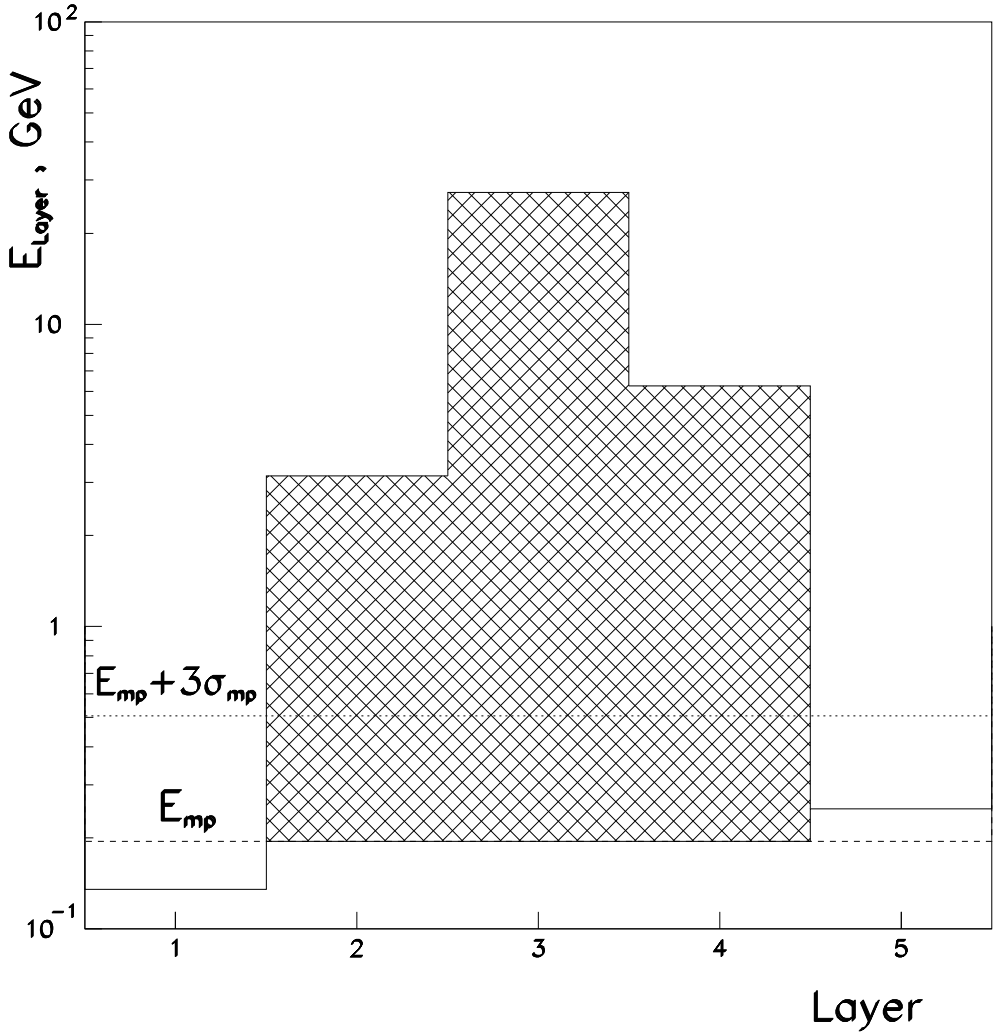

Fig. 3

Example of a 36 GeV electromagnetic shower as seen in the data. The energy E_{shower} is the sum of energies in three consecutive layers (2nd to 4th) with the signal above $E_{mp}+3\sigma_{mp}$ and with the most probable muon signal E_{mp} subtracted. The arrow corresponds to the direction of the incident muon.

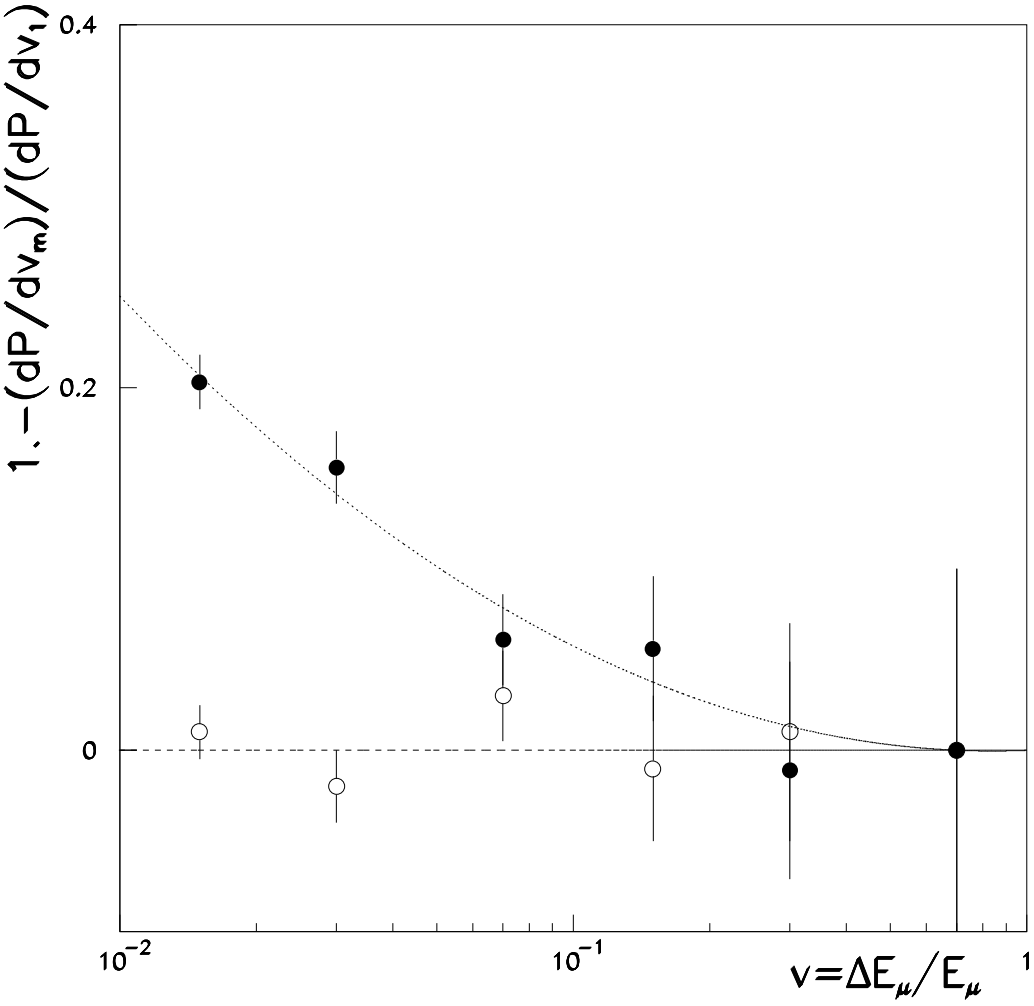

Fig. 4

Monte Carlo study of the multiple shower contribution to the differential probability distribution dP/dv. The full circles correspond to fractional losses defined as $v_m = (\Delta E_\mu - E_{m.p.})/E_\mu$, empty circles are for $v_m = (\Delta E_\mu - 1.6 \cdot E_{m.p.})/E_\mu$. The energy loss in one radiative or knock-on process is defined as $v_1 = \Delta E_{max}/E_\mu$ with ΔE_{max} being the largest energy loss in one iron slab ($0.8\ X_0$) in each muon traversal of the calorimeter.

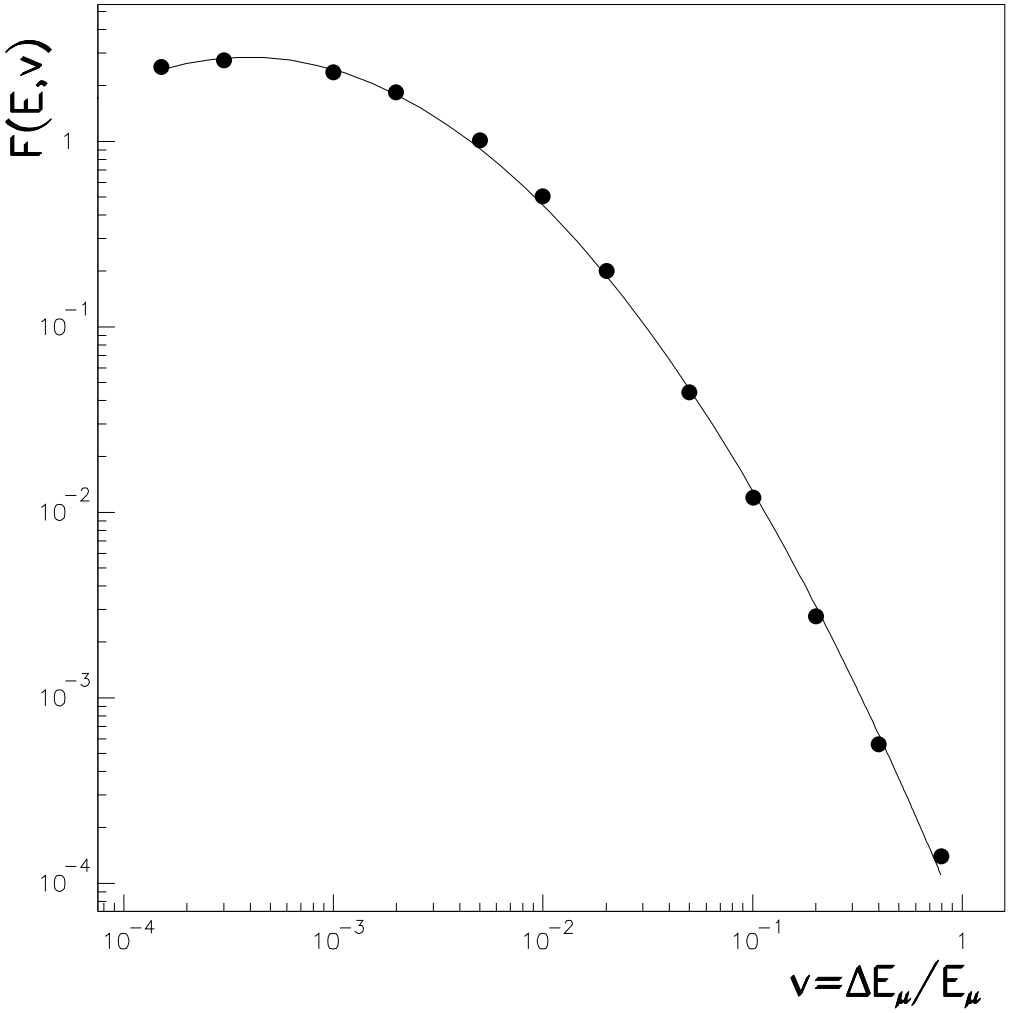

Fig. 5

The function $F(E_\mu, v)$ (see formula (1) in the text) for e^+e^- pair production by 150 GeV muons in iron. The points has been obtained by interpolation of values tabulated in Ref. [16].

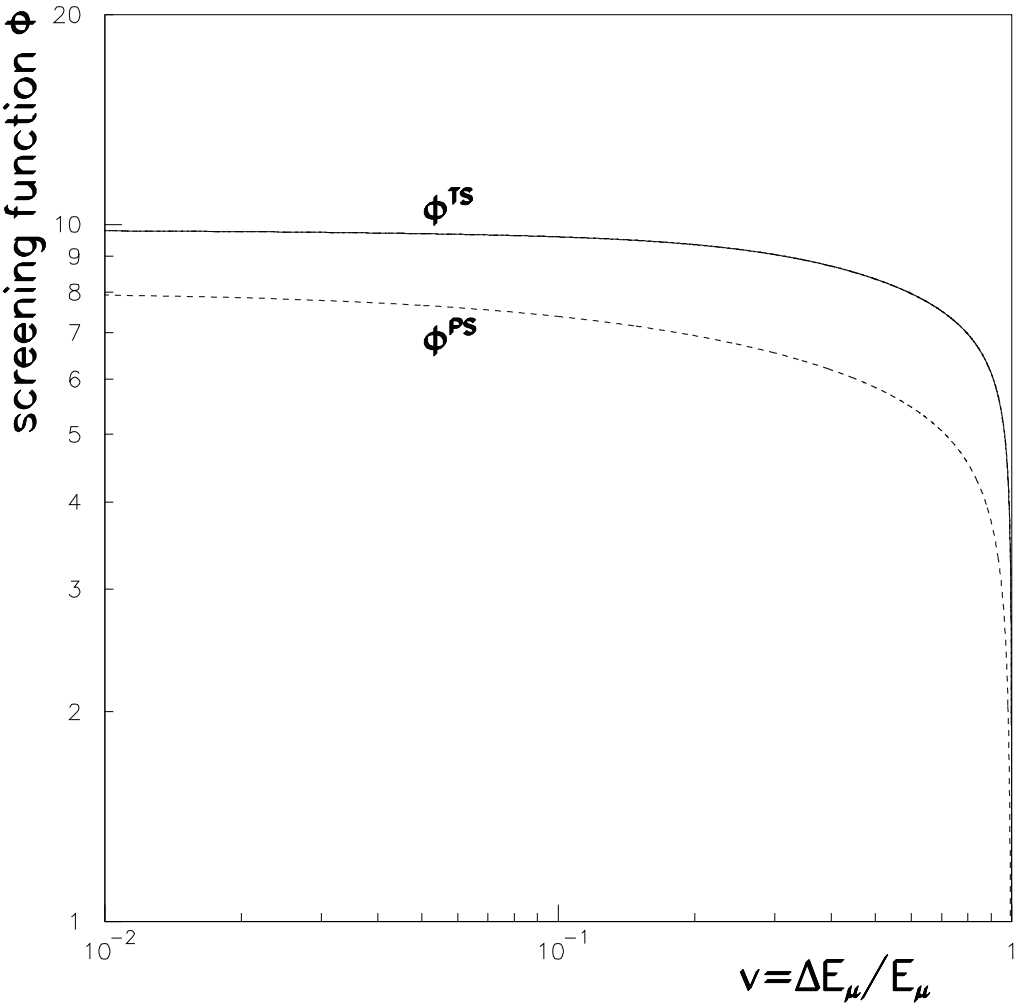

Fig. 6

Comparison of screening functions of Petrukhin and Shestakov (Φ^{PS}) and Tsai's (Φ^{TS}) description of bremsstrahlung of 150 GeV muons in iron.

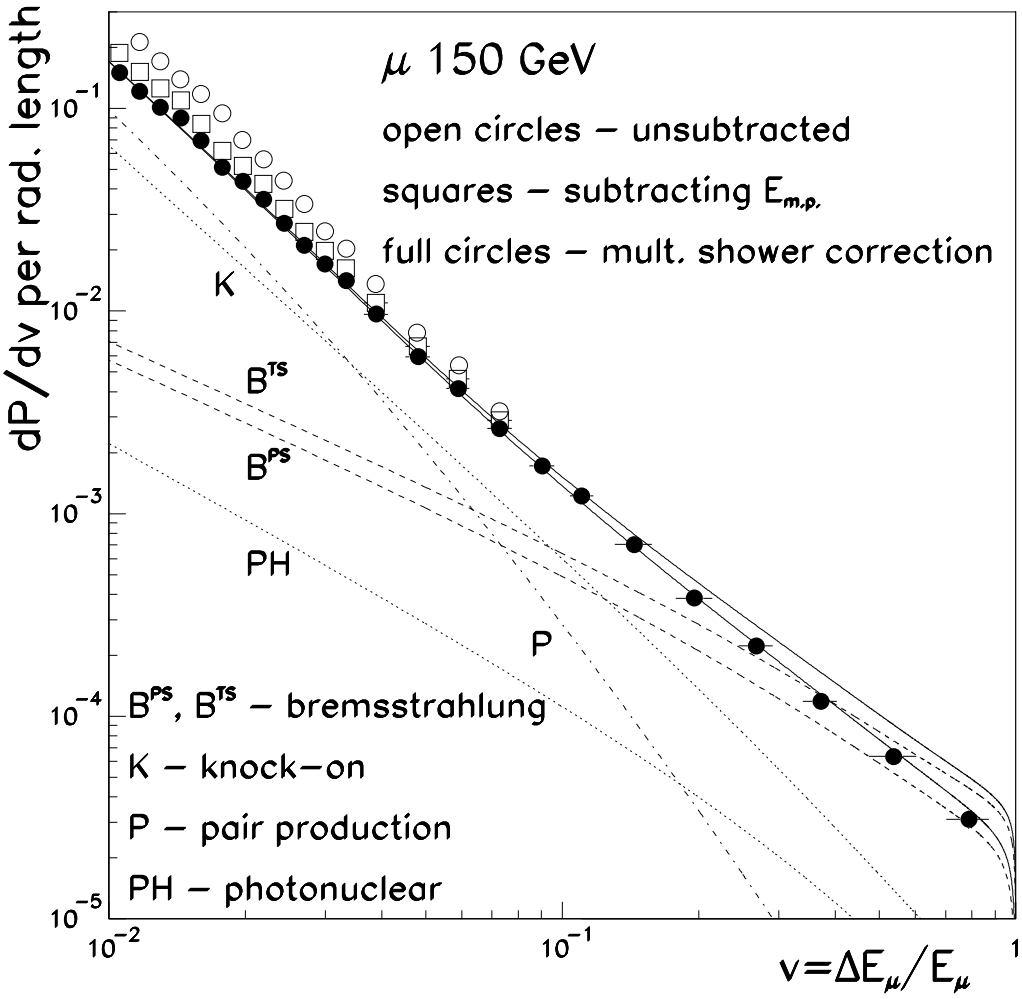

Fig. 7

The distribution of differential probabilities dP/dv for the energy loss of 150 GeV muons in iron. The curves P, K and B^{PS}, B^{TS} for pair production, knock-on electrons production and bremsstrahlung correspond to eq. (1), (2), (3) and (5) in the text. The full curves are the sum of P, K and B^{PS} (lower one) and P, K and B^{TS} (upper one). The contribution of the energy loss due to photonuclear reactions (PH) is also shown.

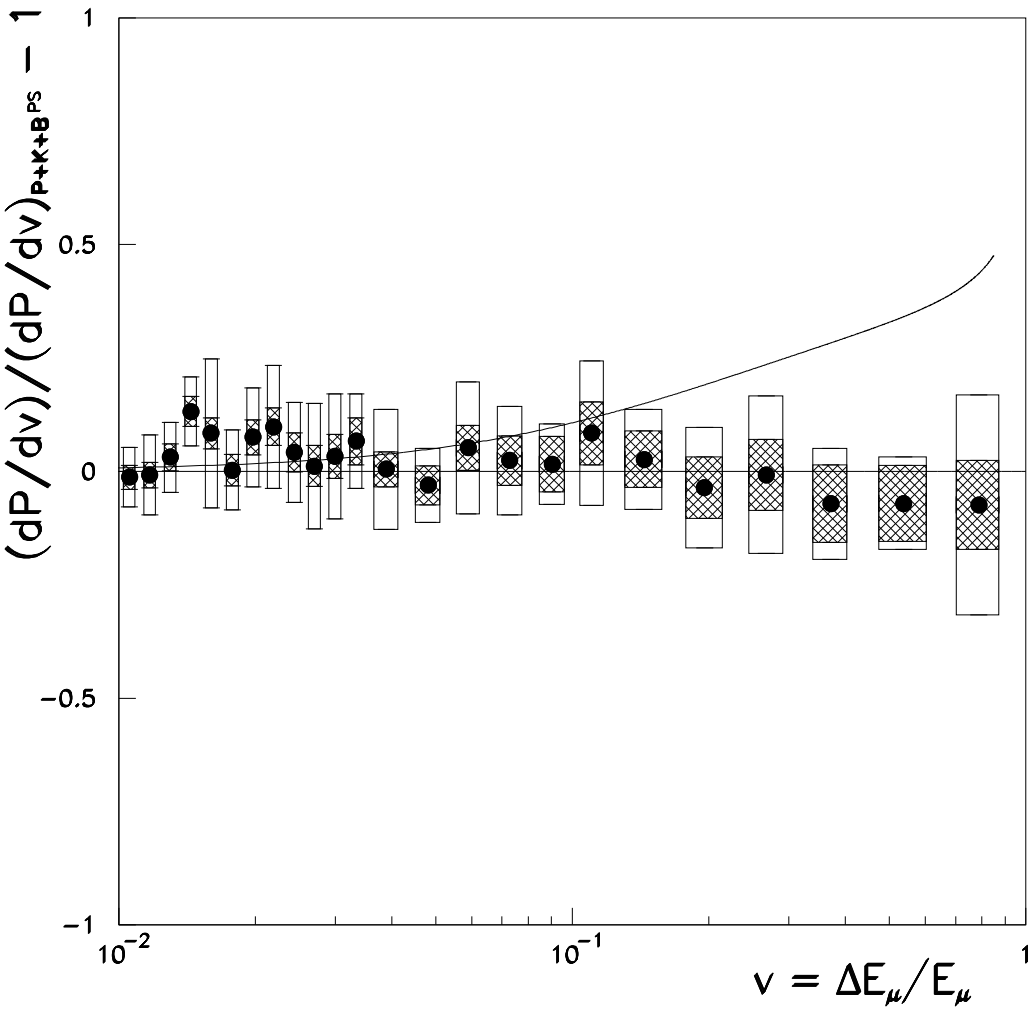

Fig. 8

Detailed comparison of the data and theory with the Petrukhin and Shestakov description of bremsstrahlung. Hatched and empty rectangles correspond to statistical and systematic errors respectively. The upper curve is the theoretical prediction with Tsai's formula for bremsstrahlung.

(v_{min}, v_{max})	$\Delta P_{measured}$	$\Delta P_{P+K+B^{PS}}$	$\Delta P_{P+K+B^{TS}}$
$(0.01, 0.03)$	$(1.180 \pm 0.010_{stat.} \pm 0.080_{syst.}) \cdot 10^{-3}$	$1.133 \cdot 10^{-3}$	$1.150 \cdot 10^{-3}$
$(0.03, 0.12)$	$(3.130 \pm 0.060_{stat.} \pm 0.190_{syst.}) \cdot 10^{-4}$	$3.039 \cdot 10^{-4}$	$3.223 \cdot 10^{-4}$
$(0.12, 0.95)$	$(1.160 \pm 0.040_{stat.} \pm 0.075_{syst.}) \cdot 10^{-4}$	$1.185 \cdot 10^{-4}$	$1.472 \cdot 10^{-4}$
$(0.01, 0.95)$	$(1.610 \pm 0.015_{stat.} \pm 0.105_{syst.}) \cdot 10^{-3}$	$1.556 \cdot 10^{-3}$	$1.619 \cdot 10^{-3}$

Table 2

Integrated probabilities $\Delta P = \int_{v_{min}}^{v_{max}} \frac{dP}{dv} dv$ per radiation length measured in three different intervals (v_{min}, v_{max}) compared with theoretical calculations for the sum of pair production (P), knock-on electron production (K) and two different formulae for bremsstrahlung, (B^{PS}) and (B^{TS}) (see formulae (1),(2),(3) and (5) respectively).